Acta Spartae Vol. 3 No. 1 2017
Pages 9–12

# Quantum mechanical investigation of the inner sphere reduction of the [(NSSSN)Co(III)Cl$^{+2}$] cation and its analogs

William Smith, Thomas Jackman[1], and Olaseni Sode[1]

Department of Chemistry, Biochemistry and Physics, University of Tampa, Tampa, FL 33606, [1]Faculty Advisor

## ABSTRACT

The inner sphere pathway is an electron transfer (ET) mechanism that utilizes a bridging ligand to covalently link oxidant and reductant centers. The reductions of chloro-N-methyl-bis(5-amino-3-thiapentyl)amine cobalt(III) [(NSNSN)Co(III)Cl$^{+3}$] and chloro(1,11-diamino-3,6,9-trithiaundecane)cobalt(III) cation [(NSSSN)Co(III)Cl$^{+2}$] by iron(II) via inner sphere ET have been shown experimentally to occur with rate constants more than $10^7$ times faster than the nitrogen analog [(NNNNN)Co(III)Cl$^{+2}$]. It has been hypothesized that this is due to non-bridging ligand effects. To test this hypothesis, the role of ground state electronic effects by the sulfur-containing ligands on the ET is investigated through the use of quantum chemistry methods. The non-bridging ligand effects were explored through the structural parameters of the cobalt complexes and by examining the LUMOs using both wavefunction theory (WFT) and density functional theory (DFT) methods. We show that the complexes containing sulfur atoms (NSSSN and NSNSN) display similar geometries. These are in contrast to the nitrogen analog (NNNNN) geometry, pointing towards a possible structural driving force in the rate constant difference.

## 1 INTRODUCTION

Electron transfer (ET), the transition of an electron from one atom to another, is a fundamental process in many chemical reactions (Marcus, 1993). It is often a foundation for determining reaction mechanisms, and is essential to understanding concepts in fields including biochemistry, organic synthesis, and solar energy. Novel examples of ET include the reduction of the heme center during respiration, and the generation of radicals and carbanions for organic synthesis. Furthermore, ET has also pushed the development of transition state theory to predict chemical rate constants (Dai et al., 2008; Hasegawa et al., 1999; Hush, 1961).

In 1951, Henry Taube described two unique ET pathways, outer sphere and inner sphere (Taube, 1952). Outer sphere electron transfer refers to the transition of the electron through the solvent, which causes the distortion of the oxidant and reductant structures during the oxidation state change (Swaddle, 1996). Inner sphere ET is mediated by a binding ligand that covalently connects two metal complexes. Thus, an excited electron can be transferred across this bridge (Mukherjee at al., 2008). In the half-century since Taube's interpretation, there have been continual experimental investigations aimed at understanding the factors that affect ET reaction rates (Rotzinger, 2014, 2015; Worrell, 1971). Initial results have shown a strong dependence on the choice of binding ligand, as well as on how labile or inert the metal complexes are.

Later, experimental studies have directed their attention to the effects of the non-bridging ligands in the inner sphere ET process. Specifically, J. Worrell and coworkers first measured the reaction rates for the Fe(II) reduction of a chloride-cobalt(III) bridge with trans located thioether and amino ligands; Equations 1, 2, and 3 respectively (Korp et al., 1983).

The structures are shown in Fig. 1. These experimental studies found that the thioether complex (Fig. 1a) and alternating ligand complex (Fig. 1b) had a reaction rate of roughly seven orders of magnitude greater than the nitrogen analog (Fig. 1c), shown in Table 1. Three possible explanations for the rate differences were a structural driving force, ground state electronic effects, and the nature of the thioether donors (trans-ligand effect). The thioether complex was examined via X-ray crystallography to determine stereochemistry and electronic ground state effects. The investigation concluded that the non-bridging ligand did not cause significant structural distortion, however was inconclusive in determining an electronic ground state effect, stating, "The possible role of ground state electronic effects, especially in sulfur-containing ligands such as NSSSN, NSNSN and NSSSN awaits theoretical and/or photochemical investigation."

In the current study, inner sphere ET across the bridging chloride atom was investigated using theoretical chemistry methods to calculate and analyze the role of electronic, trans-ligand, and structural effects in all three cobalt coordination complexes. The geometry of each complex was optimized to its lowest energy confirmation, and the wavefunctions were visualized to determine the role the highest occupied molecular orbital (HOMO) and the lowest occupied molecular orbital (LUMO) play in ground state electronic effects, and ultimately in the inner sphere reaction rate.

| Structure | Rate Constant ($M^{-1}\,s^{-1}$) |
|---|---|
| NSSSN | 0.193 |
| NSNSN | 0.226 |
| NNNNN | $1 \times 10^{-8}$ |

**Table 1.** Experimental rate constants for the three cobalt complexes (Korp et al., 1983)

$$[(\mathrm{NSSSN})\mathrm{Co(III)Cl}^{+2}] + \mathrm{Fe(II)(H_2O)_6} \longrightarrow [(\mathrm{NSSSN})\mathrm{Co(II)}^{+2}] + \mathrm{Fe(III)(H_2O)_5Cl} \quad (1)$$

$$[(\mathrm{NSNSN})\mathrm{Co(III)Cl}^{+3}] + \mathrm{Fe(II)(H_2O)_6} \longrightarrow [(\mathrm{NSNSN})\mathrm{Co(II)}^{+3}] + \mathrm{Fe(III)(H_2O)_5Cl} \quad (2)$$

$$[(\mathrm{NNNNN})\mathrm{Co(III)Cl}^{+5}] + \mathrm{Fe(II)(H_2O)_6} \longrightarrow [(\mathrm{NNNNN})\mathrm{Co(II)}^{+5}] + \mathrm{Fe(III)(H_2O)_5Cl} \quad (3)$$

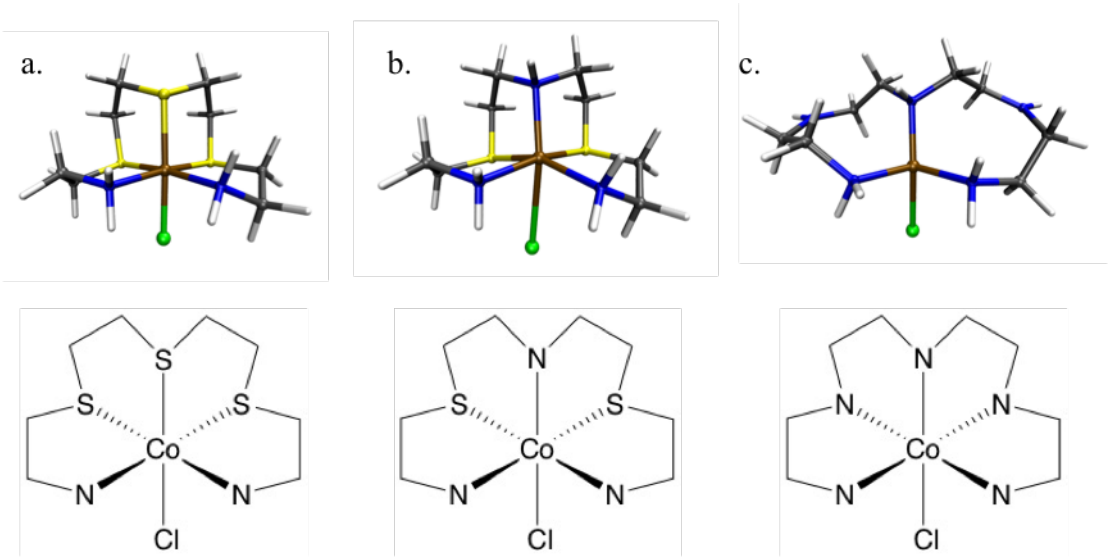


**Fig. 1.** The structures of the three cobalt complexes are shown. The CPK (top) and ChemDraw (bottom) structures are presented for the thioether ligand (NSSSN) complex (a), the alternating (NSNSN) ligand complex (b), and the nitrogen (NNNNN) ligand complex (c).

| Theory | L-Co Length (Å) | Co-CL Length (Å) | Bond Angle |
|---|---|---|---|
| B3LYP/6-31G* | 2.20 | 2.26 | 177.32° |
| PBE/6-31G* | 2.26 | 2.25 | 177.76° |
| PBE/def2-SVP | 2.31 | 2.29 | 177.86° |
| PBE/def2-TZVP | 2.26 | 2.26 | 176.91° |

**Table 2.** The DFT optimized structural parameters involved in electron transfer. The trans-ligand to metal distance (L-Co), metal to bridging-ligand (Co-Cl) distance, and the (L-Co-Cl) bond angle for the NSSSN complex are presented. Distances are shown in angstroms, angles in degrees.

| Theory | L-Co Length (Å) | Co-CL Length (Å) | Bond Angle |
|---|---|---|---|
| PBE/6-31G* | 2.59 | 2.09 | 173.92° |
| PBE/def2-SVP | 3.17 | 2.12 | 160.98° |
| PBE/def2-TZVP | 3.20 | 2.00 | 160.21° |

**Table 3.** The DFT optimized structural parameters involved in electron transfer. The trans-ligand to metal distance (L-Co), metal to bridging-ligand (Co-Cl) distance, and the (L-Co-Cl) bond angle for the NSNSN complex are presented. Distances are shown in angstroms, angles in degrees.

## 2 METHODOLOGY

Electronic structure calculations were performed using the GAMESS software package (Schmidt et al., 1993). Both wavefunction theory (WFT) and density functional theory (DFT) methods were employed at the Hartree-Fock (HF) level of WFT,

| Theory | L-Co Length (Å) | Co-CL Length (Å) | Bond Angle |
|---|---|---|---|
| PBE/6-31G* | 1.95 | 1.90 | 118.56° |
| PBE/def2-SVP | 2.01 | 1.94 | 128.47° |
| PBE/def2-TZVP | 1.97 | 1.93 | 121.03° |

**Table 4.** The DFT optimized structural parameters involved in electron transfer. The trans-ligand to metal distance (L-Co), metal to bridging-ligand (Co-Cl) distance, and the (L-Co-Cl) bond angle for the NNNNN complex are presented. Distances are shown in angstroms, angles in degrees.

Both wavefunction theory (WFT) and density functional theory (DFT) methods were employed at the Hartree-Fock (HF) level of WFT, and using the B3LYP, PBE, and LC-BOP functionals in DFT. The 6-31G* Pople basis set, and the def2-SVP and def2-TZVP Karlsruhe basis sets were employed due to their polarization-consistent parameterization and multi-function representation of wavefunctions (Bauschlicher, 2016; Witte et al., 2016). The original structure of the [(NSSSN)$CoCl^{+2}$] complex was obtained from the Cambridge Crystallographic Data Centre, and the amino groups were produced by substitution of sulfur by NH. The initial geometries were optimized at the HF level of theory. The resultant optimized HF geometry was then used as starting point for the DFT optimizations. These were calculated using spin unrestricted DFT, and in all cases the high-spin electron configuration was used. The initial optimizations of the bridged-intermediate were attempted using long-range correctional functionals (i.e. LC-BOP). In order to assess the likelihood of ET in the different complexes the optimized molecular orbitals were obtained from the optimized complex geometry. The software package Visual Molecular Dynamics (VMD) (Humphrey et al., 1996) was used to visualize the HOMO and LUMO electron densities.

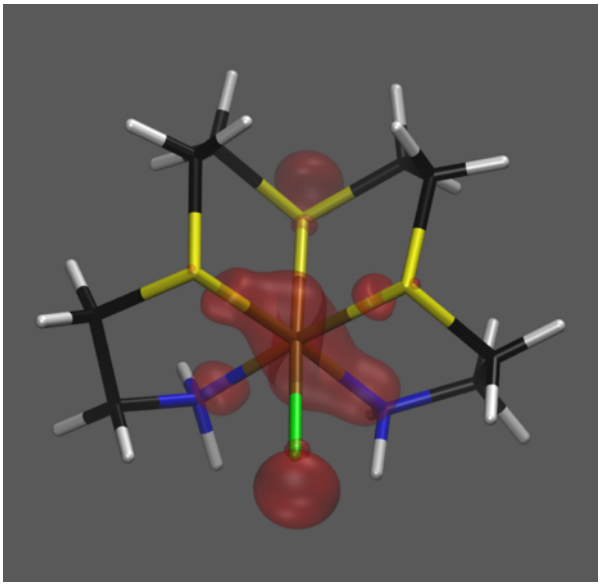

**Fig. 2.** Lowest unoccupied molecular orbital of the NSSSN complex calculated using the PBE/def2-TZVP level of theory.

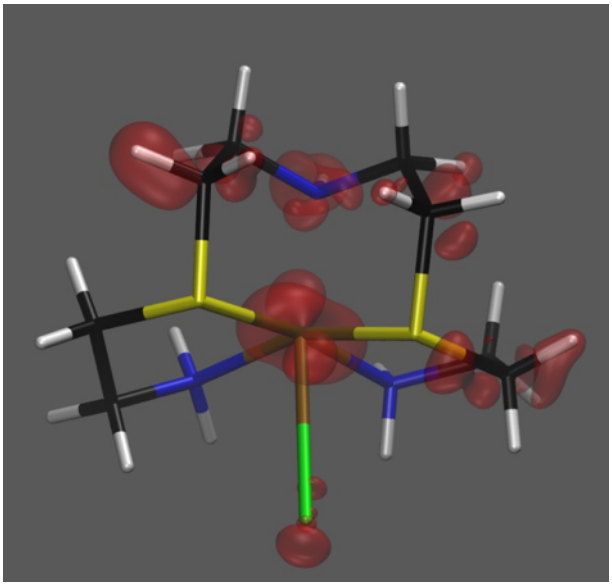

**Fig. 3.** Lowest unoccupied molecular orbital of the NSSSN complex calculated using the PBE/def2-TZVP level of theory.

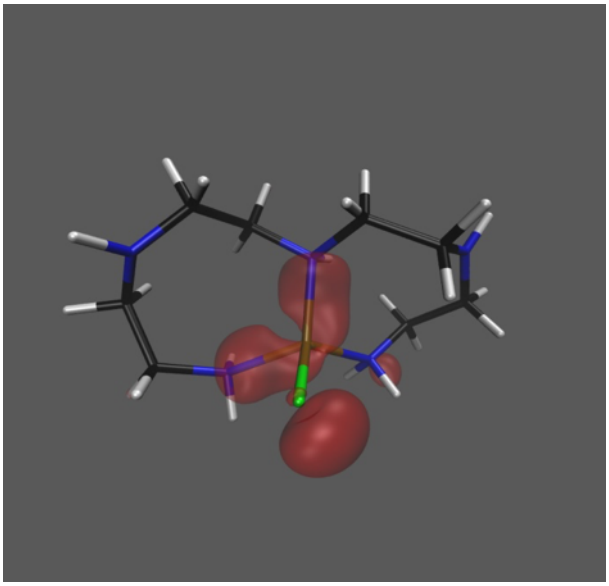

**Fig. 4.** Lowest unoccupied molecular orbital of the NSSSN complex calculated using the PBE/def2-TZVP level of theory.

## 3 RESULTS AND DISCUSSION

### Structural Driving Force

The cobalt coordination complexes were optimized using various WFT and DFT methods along with a variety of basis sets. The lowest energy configurations for the thioether, alternating, and nitrogen analog ligands at the PBE/def2-TZVP are presented in Figures 2–4, respectively. A significant structural difference between the nitrogen analog and the other two complexes was observed in these optimized geometries. The NNNNN analog was distorted in an almost planar structure compared to the NSNSN and NSSSN complexes. In these latter two, the octahedral skeleton was preserved with only minor distortions. The figures also show a slightly more acute angle for the alternating ligand complex compared to the thioether complex. The trans-ligand-cobalt-chloride (L-Co-Cl) bond angle was also measured and presented in Tables 2-4 for each complex. As expected from the structural distortions, the PBE/def2-TZVP optimization of the nitrogen analog complex shows a very acute angle at 121.0°. The angle is more obtuse in the alternating ligand complex (160.2°), and is almost linear for the thioether (176.9°). These angles between these species provide additional information in the possible electron probability overlap.

The bond lengths between the cobalt centers and the bridging chlorides, and between the cobalt centers and the *trans*-ligands were also explored (shown in Tables 2–4), since these directly relate to the ET mechanism. The Co-Cl bond length provides an initial estimation of the degree of orbital overlap essential for the ET. The distance to the *trans*-ligand also gives an initial assessment of the possible orbital overlap that may affect the ET rate. At the PBE/def2-TZVP level of theory, the Co-Cl distances for each structure are very similar. The values range from 1.93 Å to 2.26 Å. The values at the other levels of theory are also in the same range. The range of distances for the L-Co bond is, however, broader. The shortest value is for the nitrogen analog structure at 1.97 Å, followed by the thioether complex at 2.26 Å. The alternating ligand distance is even longer at 3.20 Å.

Understanding the structural differences between the complexes is important since electron transfer rates typically decrease with increasing distances between the donor and acceptor. Moreover, it is understood that similar bonding features and chelate structure

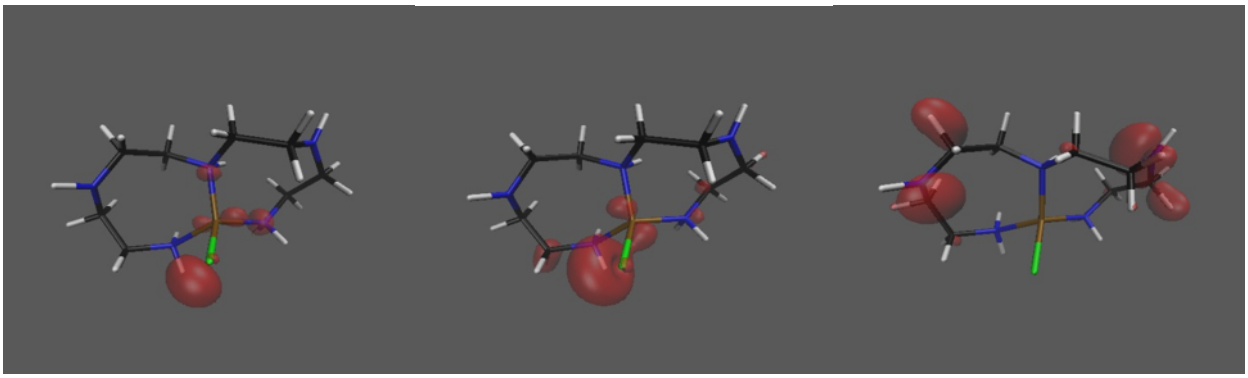

**Fig. 5.** Lowest unoccupied molecular orbital of the NSSSN complex calculated using the PBE/def2-TZVP level of theory.

tend to exhibit similar reaction rates (Worrell et al., 1979). Nonetheless, conclusive rate constant explanations necessitate explicit characterization of the electronic structure.

### Ground State Electronic/Trans-ligand Effects

The molecular orbitals for the structures optimized at the PBE/def2-TZVP level were visualized using VMD. The electron density probability distributions for the LUMOs are shown in Figures 2–4. These orbitals are important since they receive the potentially excited electron from the iron ion. Determining the spatial orientation of this orbital is important in examining the ease of ET. In agreement with the structural results, the thioether and alternating ligand complexes have similar LUMO electron densities. A larger LUMO electron density near the trans-ligand is suspected to facilitate ET and to exhibit a large rate constant. However, the nitrogen analog complex has a significantly higher electron density than the other complexes, complicating our analysis. The nitrogen analog ligand complex has a significantly different LUMO electron density. There is high electron probability all along the L-Co-Cl bond, whereas the electron probability is located only on the bridging and trans-ligand, as well as on the cobalt center in the thioether and alternating ligand complexes.

The inconsistency between orbital electron density and the ET rate constant relationship possibly stems from two sources. The first is that the nitrogen analog complex had three degenerate highest occupied molecular orbitals (Fig. 5). The degeneracy of these orbitals may suggest that one of the orbitals is involved in the electron accepting mechanism and therefore there is minimal probability overlap, following the aforementioned trend. The alternative is that the orbital transferring and the orbital accepting the electron need to be of similar energies and therefore the nitrogen analog LUMO may have a much different energy causing a decrease of ET rate. However, without an investigation into the Co-Fe transition state structure, it is difficult to make predictions about potential rate constants or explanations.

## 4 SUMMARY

The minimum energy geometries of three cobalt coordination complexes (NSSSN, NSNSN, NNNNN) were determined using electronic structure methods. The similarities in the structures of the thioether and alternating complexes support the experimental rate constant. Likewise, the nitrogen analog, with a nearly inert rate constant, showed significant structural changes when compared to the other complexes. In addition, electronic ground state effects were investigated by visualizing the molecular orbitals. Again, the thioether and alternating ligand complexes had similar electronic structure; however, the nitrogen analog complex showed unexpected electron density. Future work will focus on the intermediate-bridged complex between the reduced cobalt and oxidized iron center. Optimizations of the ground and first excited state of the bridged complex transition structures will enable the determination of the theoretical rate constants using Marcus theory. Similar ligands will be investigated, hopefully forgoing extensive synthesis procedures.

## REFERENCES


Bauschlicher Jr., C. W. 2016, Chem Phys Lett 665:100-104

Dai, Z., Bai, H., Hong, M., Zhu, Y., Bao, J. & Shen, J. 2008, Biosens Bioelectron 23(12):1869–1873

Hasegawa, E., Yoneoka, A., Suzuki, K., Kato, T., Kitazume, T. & Yanagi, K. 1999, Tetrahedron 55:12957–12968

Humphrey, W., Dalke, A. & Schulten, K. 1996, J Mol Graphics 14(1):33–38

Hush, N. S. 1961, Trans Faraday Soc 57:557–580

Korp, J. D., Bernal, I. & Worrell, J. H. 1983, Polyhedron 2(5):323–330

Marcus, R. A. 1993 Angew Chem Int Ed 32(8):1111–1121

Mukherjee, A., Smirnov, V. V., Lanci, M. P., Brown, D. E., Shepard, E. M., Dooley, D. M. & Roth, J. P. 2008, J Am Chem Soc 130(29):9459–9473

Rotzinger, F. P. 2014, Inorg. Chem. 53(18):9923-9931

Rotzinger, F. P. 2015, Inorg Chem 54(21): 10450–10456

Schmidt, M. W., Baldridge, K. K., Boatz, J. A., Elbert, S. T., Gordon, M. S., Jensen, J. H., Koseki, S., Matsunaga, N., Nguyen, K. A., Su, S., Windus, T. L., Dupuis, M. & Montgomery, J. A. 1993, J Comput Chem 14(11):1347–1363

Swaddle, T. W. 1996, Can J Chem 74(5):631–638

Taube, H. 1952, Chem Rev 50(1):69-126

Witte, J., Neaton, J. B. & Head-Gordon, M. 2016, J Chem Phys 144:194306

Worrell, J. H., Goddard, R. & Jackman, T. 1979, Inorg Chim Acta 32:L71–L73

Worrell, J. H. & Jackman, T. A. 1971, J Am Chem Soc 93(4):1044–1046